

# Design of Miniaturized SIW Diplexers with Low Insertion Loss and High Isolation

Ya-Na Yang, Guo Hui Li\*, Li Sun, Xiu-Guang Chen, and Xue-Xia Yang

**Abstract**—This paper presents two novel substrate integrated waveguide (SIW) diplexers with transmission zeros placed below and above the passband. Diplexer I is based on two bandpass filters (BPFs) using eighth mode SIW (EMSIW) cavities with Rx and Tx frequencies at 3.68 GHz and 6.09 GHz. The second one is operated at 2.37 GHz and 6.04 GHz using EMSIW and thirty-second SIW (TMSIW) cavity. The diplexers are all combined through a T-junction by carefully choosing the length and width of two branches to allow each filter to match the antenna, while maintaining an open circuit at the middle band of the other. The proposed diplexers possess compact size, because of the EMSIW and TMSIW cavity. The diplexers are fabricated in SIW technology. The minimum insertion losses including SMA connectors are measured to be 1.39/1.61 dB and 0.38/0.85 dB. Meanwhile, the diplexers exhibit 37 dB and 42 dB isolations between the channels, respectively. Good agreement is achieved between simulated and measured results.

## 1. INTRODUCTION

Diplexers are essential components in the modern wireless communication system to effectively separate transmit and receive channels connected to a common antenna. Diplexers play an important role in improving the performance of the entire communication system, therefore, the demand for the design diplexers of compact size, low insertion loss, high isolation and high-performance is increasing over the last few decades. The SIW technique exhibits some advantages such as low loss, compact size, high Q-factor and easy integration, which makes it to be widely used in the design of the diplexer. In [1], a compact SIW diplexer based on circular triplet combline triplets was proposed and demonstrated at X-band. A miniaturized SIW diplexer loaded by CSRRs was proposed in [2], and it was operated below the waveguide cutoff.

Since the diplexer consists of two filters operating at two different frequencies, the simplest way to reduce the size of the diplexer is miniaturizing both filters. However, for highly integrated microwave components, the SIW resonator is still relatively large. In order to further reduce the size of the circuit while maintaining the good performance characteristics of SIW, several improvements have been proposed. Wei Hong et al. proposed a new guided wave structure: half mode SIW (HMSIW) in 2006 [3]. After that, several structures have been developed by cutting the SIW resonators on fictitious magnetic walls to achieve quarter mode SIW (QMSIW), eighth mode SIW (EMSIW), sixteenth mode SIW (SMSIW) or even thirty-second mode SIW (TMSIW) [4–6].

In this paper, two compact diplexers are proposed. Both diplexers are composed of two BPFs, which are connected to the common input port through a microstrip T-junction. The first diplexer is based on EMSIW cavities and diplexer II is formed by exploiting EMSIW and TMSIW cavities to meet various requirements, respectively. Both diplexers are analyzed and designed using full-wave

---

*Received 6 July 2018, Accepted 16 August 2018, Scheduled 24 August 2018*

\* Corresponding author: Guo Hui Li (ghlee@sohu.com).

The authors are with the Key Laboratory of Specialty Fiber Optics and Optical Access Network, Shanghai University, Shanghai 200072, China.

EM simulator software (Ansys HFSS). The diplexers are also fabricated on a Rogers RT/Duroid 5880 substrate with a thickness of 0.508 mm and then measured by Agilent N5227A network analyzer. The experimental and simulated results are provided with careful comparison and good agreements.

## 2. DIPLEXER DESIGN

### 2.1. EMSIW Cavity

The magnitudes of the simulated electric field in the square SIW, HMSIW, QMSIW and EMSIW cavities resonating at the dominant mode  $TE_{101}$  are depicted in Fig. 1, respectively. Since the maximum value of the electric field when working in the dominant resonant mode is on the vertical center plane along the propagation direction, the symmetrical planes (i.e., A-A', B-B', C-C', D-D') can be regarded as perfect magnetic walls. Based on this idea, half of the SIW will keep the half field distribution unchanged by cutting the SIW resonant cavity along the plane A-A' and then the SIW becomes an HMSIW. As shown in Fig. 1(b), the similar propagation characteristics holds but the size is nearly half reduced. It is noted that the HMSIW can be bisected again along the symmetrical plane D-O, and QMSIW is realized. Then EMSIW is derived by further bisecting the QMSIW cavity along O-C', as shown in Fig. 1(d). Therefore, the overall size of EMSIW cavity can be reduced by a factor of more than 7/8 compared to the conventional SIW resonator, while keeping the resonant frequency almost unchanged.

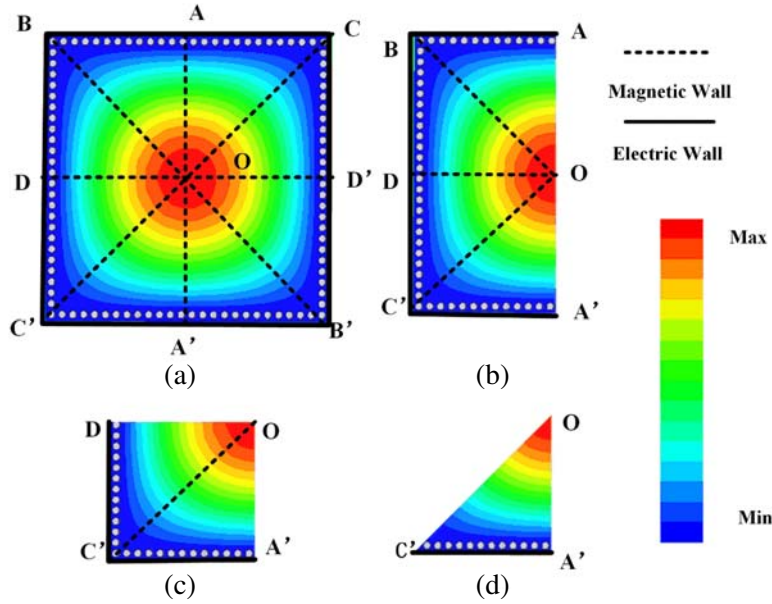


**Figure 1.** Electric field distributions of (a) full-mode SIW, (b) HMSIW, (c) QMSIW, (d) EMSIW.

The resonant frequency of the dominant mode  $TE_{101}$  can be determined by Eq. (1) [7] as follows:

$$f = \frac{c}{2\pi\sqrt{\mu_r\epsilon_r}} \sqrt{\left(\frac{\pi}{a_{eff}}\right)^2 + \left(\frac{\pi}{b_{eff}}\right)^2} \quad (1)$$

where  $a_{eff}$  and  $b_{eff}$  are the equivalent length and width of the rectangular SIW cavity;  $\mu_r$  and  $\epsilon_r$  are the relative permeability and relative dielectric constant, respectively;  $c$  is the speed of light in free space.

### 2.2. Bandpass Filter Design

The configuration of the BPF using EMSIW cavities is shown in Fig. 2(a). Two intersecting rectangular slots are etched between the two cavities, where the angle between the two slots is  $30^\circ$ . The slots are

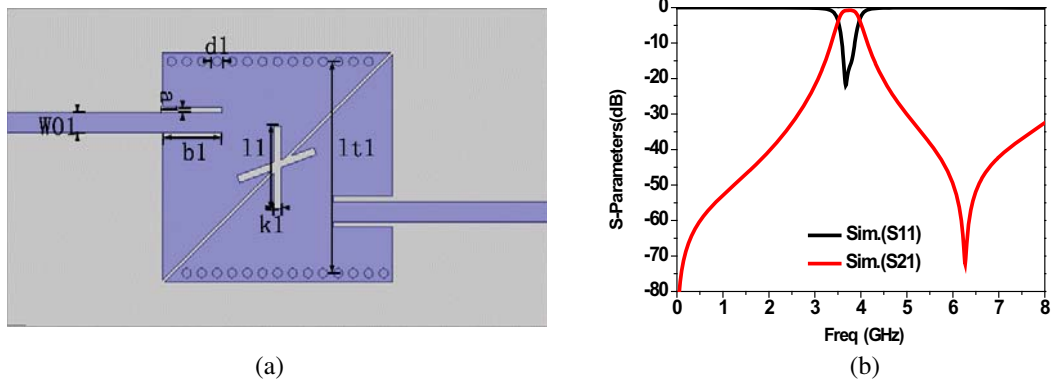


**Figure 2.** (a) Configuration of the BPF and (b) simulated frequency responses of the BPF.

used to couple energy from one cavity to another and they can also create a TZ at upper band. Two  $50\ \Omega$  microstrip lines through a pair coplanar waveguides are adopted as input/output ports. Fig. 2(b) shows the simulated  $S$ -parameters of the proposed BPF. It can be seen that its center frequency is at 3.75 GHz with insertion loss of 0.77 dB, and the passband return loss is better than 21 dB. One transmission zero is located at 6.27 GHz above the passband, and the location of the TZ can be controlled by changing the dimension of the slots, so the stopband rejection in the upper band of this filter is greatly improved.

### 2.3. Diplexer Structure

As shown in Fig. 3, diplexer I is composed of two proposed channel filters discussed above, where two filters are connected to a common input port through microstrip T-junction. A metallic via is implemented on one of the cavities of the upper-band filter, which is used to suppress the influence of upper-band filter on the passband of lower-band channel to improve the isolation of the two channel filters. In our previous work [6], a novel BPF using TMSIW cavity is proposed. Based on the EMSIW cavity filter and the TMSIW cavity filter, Fig. 4 shows the configuration for diplexer II with a transmitter filter and a receiver filter cascaded inline. The T-junction is the most common method of combining two filters together. Therefore, two BPFs are combined using a simple T-junction, which is used to reduce the interaction of the two BPFs to improve the isolation. After obtaining two filters with desirable performance, the passband feature of both filters connected with a T-junction will be affected. To avoid this problem, the length and width of the two branches of the T-junction must be chosen carefully. In order to obtain the expected performance, all the parameters in Fig. 3 and Fig. 4 are optimized using full-wave EM simulator software (Ansys HFSS). The final optimized parameters of the diplexers are:  $W01 = 1.3\ \text{mm}$ ,  $d1 = 0.6\ \text{mm}$ ,  $a1 = 0.4\ \text{mm}$ ,  $b1 = 4\ \text{mm}$ ,  $lt1 = 14.3\ \text{mm}$ ,  $l1 = 5.5\ \text{mm}$ ,  $k1 = 0.5\ \text{mm}$ ,  $Wz1 = 2\ \text{mm}$ ,  $W02 = 1\ \text{mm}$ ,  $d2 = 0.4\ \text{mm}$ ,  $b2 = 2.5\ \text{mm}$ ,  $a2 = 0.3\ \text{mm}$ ,  $lt2 = 10\ \text{mm}$ ,  $l2 = 3.1\ \text{mm}$ ,  $W03 = 1\ \text{mm}$ ,  $a3 = 0.3\ \text{mm}$ ,  $b3 = 2\ \text{mm}$ ,  $l3 = 3.3\ \text{mm}$ ,  $k2 = 0.5\ \text{mm}$ ,  $d3 = 0.4\ \text{mm}$ ,  $lt3 = 10\ \text{mm}$ ,  $Wz2 = 2.9\ \text{mm}$ ,  $W04 = 2.3\ \text{mm}$ ,  $a4 = 0.2\ \text{mm}$ ,  $b4 = 2\ \text{mm}$ ,  $l4 = 8.7\ \text{mm}$ ,  $k3 = 0.5\ \text{mm}$ ,  $d4 = 1\ \text{mm}$ ,  $r2 = 0.6\ \text{mm}$ ,  $lt4 = 28\ \text{mm}$ .

## 3. RESULTS AND DISCUSSION

In order to verify the accuracy of the above analysis, two diplexers are fabricated on a 0.508 mm-thick Rogers RT/Duroid 5880 substrate with the relative permittivity  $\epsilon_r = 2.2$  and dielectric loss tangent  $\tan\delta = 0.0009$ . All the circuits in this paper are measured by the Agilent N5227A vector network analyzer. Fig. 6 shows the photograph of the fabricated diplexer. Simulated and measured results are shown in Fig. 5. As we can see from Fig. 5(a), for diplexer I, the measured results are in good agreement with the simulated ones. The measured central frequencies of the TX filter and the RX filter are 3.68 GHz and 6.09 GHz. The bandwidth of the lower channel is 450 MHz, and that of the higher channel is 500 MHz. The minimum insertion losses are approximately 1.39 dB and 1.61 dB, which are

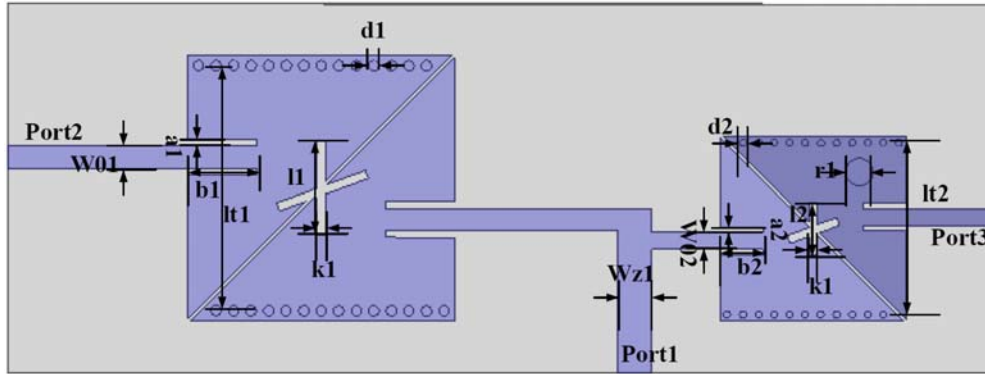


Figure 3. Configuration of the proposed diplexer I.

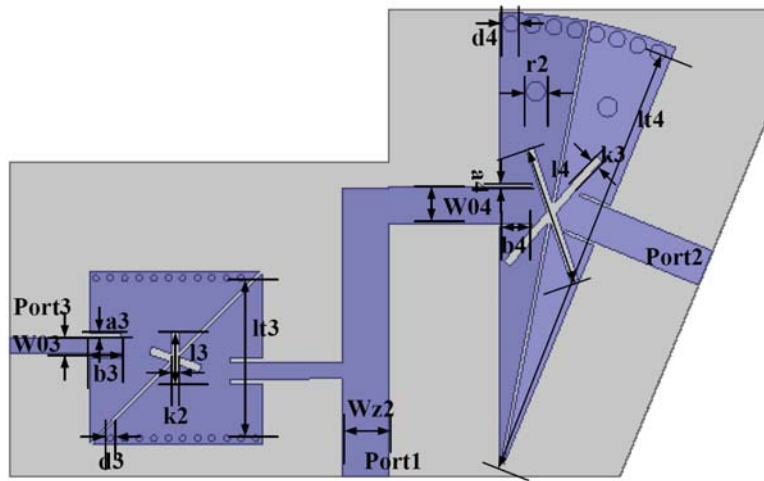


Figure 4. Configuration of the proposed diplexer II.

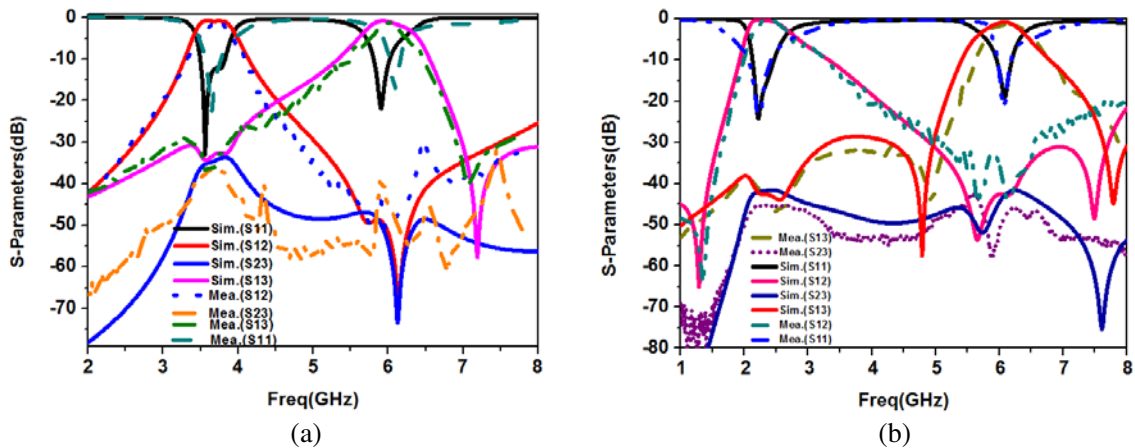
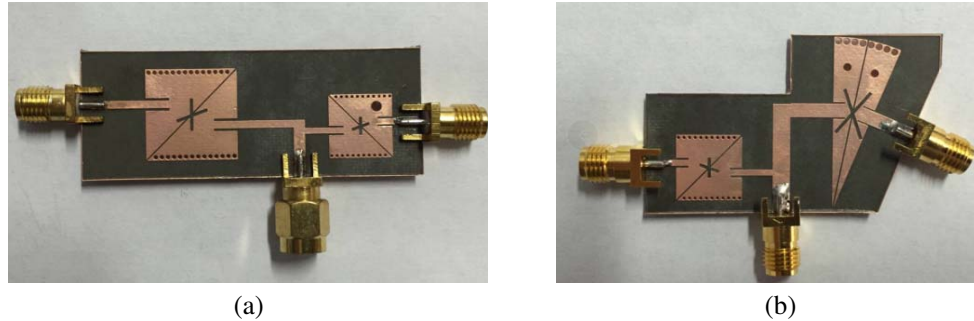


Figure 5. Simulated and measured results. (a) Diplexer I, (b) Diplexer II.

about 0.5 dB larger than the simulated predicts, while the return losses are 23 dB and 18 dB, respectively. Two transmission zeros are created at 6.15 and 7.19 GHz. The measured isolation between ports 2 and 3 is better than 37 dB. As shown in Fig. 5(b), for diplexer II the measured center frequency is at 2.37 GHz for channel 1 with the bandwidth of 600 MHz, 6.04 GHz for channel 2 with the bandwidth of

500 MHz. The minimum insertion losses are around 0.38dB and 0.85dB at the lower and upper channels respectively, which include the extra loss from the SMA connectors. The measured return losses at the lower and higher bands are better than 24 dB and 20 dB. The isolation is better than 42 dB. Multiple transmission zeros are observed due to the coexistence of electric and magnetic couplings. The total sizes of the diplexers are 21.5 mm × 57.3 mm × 0.508 mm, 47.9 mm × 29.1 mm × 0.508 mm, respectively. Comparison with other diplexers proposed in the references is listed in Table 1. From the Table, it indicates that the highest isolation of the proposed diplexers than those in [8], [9] and [10]. Moreover, diplexer II has the lowest insertion loss and relatively compact size.



**Figure 6.** Photograph of the fabricated diplexers. (a) Diplexer I, (b) Diplexer II.

**Table 1.** Comparison between the proposed diplexers and the references.

		$f_0$ (GHz)	IL (dB)	Isolation (dB)	Size ( $\lambda_g^2$ )
[8]		2.07/2.71	1.54/2	36	0.45 × 0.48
[9]		1.85/2.454	1.42/1.77	33	0.857 × 0.212
[10]		1.95/2.14	1.46/1.44	36	0.45 × 0.74
This work	Diplexer I	3.68/6.09	1.39/1.61	37	0.264 × 0.703
	Diplexer II	2.37/6.04	0.38/0.85	42	0.377 × 0.229

#### 4. CONCLUSION

In this paper, two novel diplexers using EMSIW and TMSIW cavities are presented, fabricated and measured, where two passbands are centered at 3.68/6.09 GHz and 2.37/6.04 GHz, respectively. To increase the isolation between the two filters, two BPFs of the diplexers are connected by a simple T-junction that makes the component even more compact. Among them, the diplexer II also achieves a good insertion loss and miniaturization. The measured results and simulated results are in good agreement that verifies the accuracy of the proposed design method. The diplexers have compact size, simple configuration, low-loss and ease of fabrication, which makes them suitable candidates for application in microwave communication systems.

#### ACKNOWLEDGMENT

This work is supported by the National High-tech Research Development Plan (863 Plan) (2015AA016201).

**REFERENCES**

1. Sirci, S., J. D. Martínez, J. Vague, and V. E. Boria, "Substrate integrated waveguide diplexer based on circular triplet combline filters," *IEEE Microw. Wireless Compon. Lett.*, Vol. 25, No. 7, 430–432, 2015.
2. Dong, Y. D. and T. Itoh, "Substrate integrated waveguide loaded by complementary split-ring resonators for miniaturized diplexer design," *IEEE Microw. and Wireless Compon. Lett.*, Vol. 21, No. 1, 10–12, 2011.
3. Hong, W., B. Liu, Y. Q. Wang, Q. H. Lai, H. J. Tang, X. X. Yin, Y. D. Dong, Y. Zhang, and K. Wu, "Half mode substrate integrated waveguide: A new guided wave structure for microwave and millimeter wave application," *2006 Joint 31st International Conf. on Infrared Millimeter Waves and 14th International Conf. on Terahertz Electronics*, 219–219, 2006.
4. Zhang, X. J., C. Y. Ma, and F. Wang, "Design of compact dual-passband LTCC filter exploiting stacked QMSIW and EMSIW," *Electronics Lett.*, Vol. 51, No. 12, 912–914, 2015.
5. Azad, A. R. and A. Mohan, "Sixteenth-mode substrate integrated waveguide bandpass filter loaded with complementary split-ring resonator," *Electron. Lett.*, Vol. 53, No. 8, 546–547, 2017.
6. Yang, Y. N., G. H. Li, L. Sun, W. Yang, and X. X. Yang, "Design of compact bandpass filters using sixteenth mode and thirty-second mode SIW cavities," *Progress In Electromagnetics Research Letters*, Vol. 75, 61–66, 2018.
7. Li, P., H. Chu, and R. S. Chen, "Design of compact bandpass filters using quarter-mode and eighth-mode SIW cavities," *IEEE Trans. Compon. Packag. Technol.*, Vol. 7, No. 6, 956–963, 2017.
8. Hagag, M. F., M. A. Khater, M. D. Hickie, and D. Peroulis, "Tunable SIW cavity-based dual-mode diplexers with various single-ended and balanced ports," *IEEE Trans. Microw. Theory Tech.*, Vol. 66, No. 3, 1238–1248, 2018.
9. Xue, Q., J. Shi, and J. X. Chen, "Unbalanced-to-balanced and balanced-to-unbalanced diplexer with high selectivity and common-mode suppression," *IEEE Trans. Microw. Theory Tech.*, Vol. 59, No. 11, 2848–2855, 2011.
10. Chuang, M. L. and M. T. Wu, "Microstrip diplexer design using common T-shaped resonator," *IEEE Microw. and Wireless Compon. Lett.*, Vol. 21, No. 11, 583–585, 2011.